Proc. Natl. Acad. Sci. USA
Vol. 93, pp. 9521–9526, September 1996
Biophysics

Conformational dependence of electron transfer across *de novo* designed metalloproteins

MITCHELL W. MUTZ*, GEORGE L. MCLENDON*†, JAMES F. WISHART‡, ELIZABETH R. GAILLARD§, AND ALAN F. CORIN¶

*Department of Chemistry, Princeton University, Princeton, NJ 08544; ‡Department of Chemistry, Brookhaven National Laboratories, Upton, NY 11973; §Department of Chemistry, University of Rochester, Rochester, NY 14627; and ¶Scrippgen Pharmaceuticals, Inc., 200 Boston Avenue, Medford, MA 02155

Communicated by Walter Kauzmann, Princeton, NJ, June 27, 1996 (received for review March 22, 1996)

ABSTRACT **Flash photolysis and pulse radiolysis measurements demonstrate a conformational dependence of electron transfer rates across a 16-mer helical bundle (three-helix metalloprotein) modified with a capping Co^{III}(bipyridine)$_3$ electron acceptor at the N terminus and a 1-ethyl-1′-ethyl-4,4′-bipyridinium donor at the C terminus. For the Co^{III}(peptide)$_3$-1-ethyl-1′-ethyl-4,4′-bipyridinium maquettes, the observed transfer is a first order, intramolecular process, independent of peptide concentration or laser pulse energy. In the presence of 6 M urea, the random coil bundle (≈0% helicity) has an observed electron transfer rate constant of k_{obs} = 900 ± 100 s^{-1}. In the presence of 25% trifluoroethanol (TFE), the helicity of the peptide is 80% and the k_{obs} increases to 2000 ± 200 s^{-1}. Moreover, the increase in the rate constant in TFE is consistent with the observed decrease in donor–acceptor distance in this solvent. Such bifunctional systems provide a class of molecules for testing the effects of conformation on electron transfer in proteins and peptides.**

De novo design of redox proteins represents a significant challenge for biological and biomimetic chemistry (1, 2). Several maquettes have been designed toward systems in which electrons can be translocated across proteins (3, 4). A wealth of data now exist for modified natural proteins like cytochrome *c* (5, 6). Significant data are also available for modified single peptide systems (7), but conformational equilibria often complicate the interpretation of simple systems (8). Two particularly attractive structural maquettes for the design and study of *de novo* redox proteins were reported by Ghadhiri *et al.* (9) and Lieberman and Sasaki (10). Both systems consist of a three helix bundle, whose stoichiometry and topology are defined by the capping metal bipyridyl complex. These bundles have been well characterized in the literature (2, 9–11). Because there are numerous tris-bipyridyl complexes, using this motif to create three helix bundles allows ready access to the many varied spectroscopic, photophysical, and redox properties offered by these metal compounds. Moreover, the ability to control the conformation of these three helix bundles under different solvent conditions provides a facile system in which to study the effects of secondary structure on rates of electron transfer (ET), while maintaining a constant bond connectivity. By probing the ET rates of a designed metalloprotein in both folded and unfolded states, the role of helical secondary structure in mediating ET can be investigated.

MATERIALS AND METHODS

Peptide Modifications. A minor elaboration on these metalloproteins provides a model bifunctional redox system in which redox active 1-ethyl-1′-ethyl-4,4′-bipyridinium is covalently linked to the C terminus of a bipyridine-modified 16-mer peptide, called "16-mer," and a redox active metal (cobalt) is incorporated into the N terminus as shown in Fig. 1. The sequence of the 16-mer and the structure of the C-terminal modifier, 1-ethyl-1′-ethyl-4,4′-bipyridinium, are also given in Fig. 1. The peptide was synthesized by standard solid phase methods (12). Synthesis of 4-carboxy-4′-methyl-2,2′-bipyridine and attachment of 4-carboxy-4′-methyl-2,2′-bipyridine to the N terminus of the peptide and subsequent purification proceeded according to standard procedures (10, 13). The synthesis of 1-bromoethyl-1′-ethyl-4,4′-bipyridinium has been described (14). The C terminus of the bipyridine-modified 16-mer was covalently attached to 1-ethyl-1′-ethyl-4,4′-bipyridinium by the following method: 2 mg of 16-mer (1 μmol) in 1 ml of 100 mM phosphate (pH = 8.0) was treated with 1 μmol dithiothreitol for 20 min to reduce any disulfides and 5–10 μmol of the 1-bromoethyl-1′-ethyl-4,4′-bipyridinium was added. The solution was stirred in the dark at room temperature for 18 hr, and the product was purified by solid-phase extraction in a 1:1 100 mM ammonium acetate (pH 9.0):CH_3 CN with a Sep-Pak Plus C18 Cartridge (Waters), followed by lyophilization. This was followed by reverse-phase HPLC using a Hamilton PRP-1 column with a linear gradient of 10–45% CH_3CN in 50 mM ammonium acetate (pH 9.0) over 40 min. The product elutes as a single peak at 35–37% CH_3CN. Formation of the 16-mer‖ 1-ethyl-1′-ethyl-4,4′-bipyridinium complex, hereafter referred to as 16-mer-viologen for brevity, was confirmed by absorbance spectroscopy, amino acid analysis, and mass spectroscopy.

Synthesis of Co^{III}(16-mer)$_3$-Viologen. A 1:2 16-mer:16-mer viologen was stirred for 20 min with a one-third equivalence of cobalt(II) prepared from $Co(NO_3)_2{\cdot}6H_2O$ in 100 mM potassium phosphate (pH 7.0) and then Co^{II}(16-mer)$_3$-viologen was oxidized electrochemically. The resulting complex is pale yellow with an absorbance spectrum λ_{max} (ε, M^{-1} cm^{-1}) = 308 (3.7×10^4) comparable to that of Co^{III} tris-bipyridine as shown in Fig. 2 (15). The final Co^{III}(16-mer)$_3$-viologen maquette was then purified from unreacted monomer via gel permeation on a Superose 12 HR 10/30 column (Pharmacia). Analytical gel permeation and mass spectroscopy gave no evidence of crosslinking between unmodified cysteine residues. Absorbance spectroscopy revealed an average of two viologen moieties per trimer, depending on the proportion of 16-mer:16-mer-viologen used. In addition, circular dichroism (CD) spectroscopy showed that the triple-helix 16 mer complex, Co^{III}(16 mer)$_3$-viologen, adopts the configuration already defined by the parent peptide as shown in Fig. 3 (10). Both the Co^{III} tris-bipyridine and viologen moieties of the metalloprotein readily undergo redox reactions at similar potentials to those of the isolated systems (cobalt: E° = + 0.15 V; viologen: E° = −0.64 V, both vs. saturated NaCl calomel electrode, determined by cyclic voltammetry). Voltammetric data are given in Fig. 4. The model compounds Co^{III}(4-methyl-4′-alanine-2,2′-bipyridine)$_3$ and 16-mer-viologen were used to

The publication costs of this article were defrayed in part by page charge payment. This article must therefore be hereby marked "*advertisement*" in accordance with 18 U.S.C. §1734 solely to indicate this fact.

Abbreviations: ET, electron transfer; TFE, trifluoroethanol; CD, circular dichroism.

†To whom reprint requests should be addressed.

‖Viologen is the trivial name of 4,4′-bipyridinium compounds.

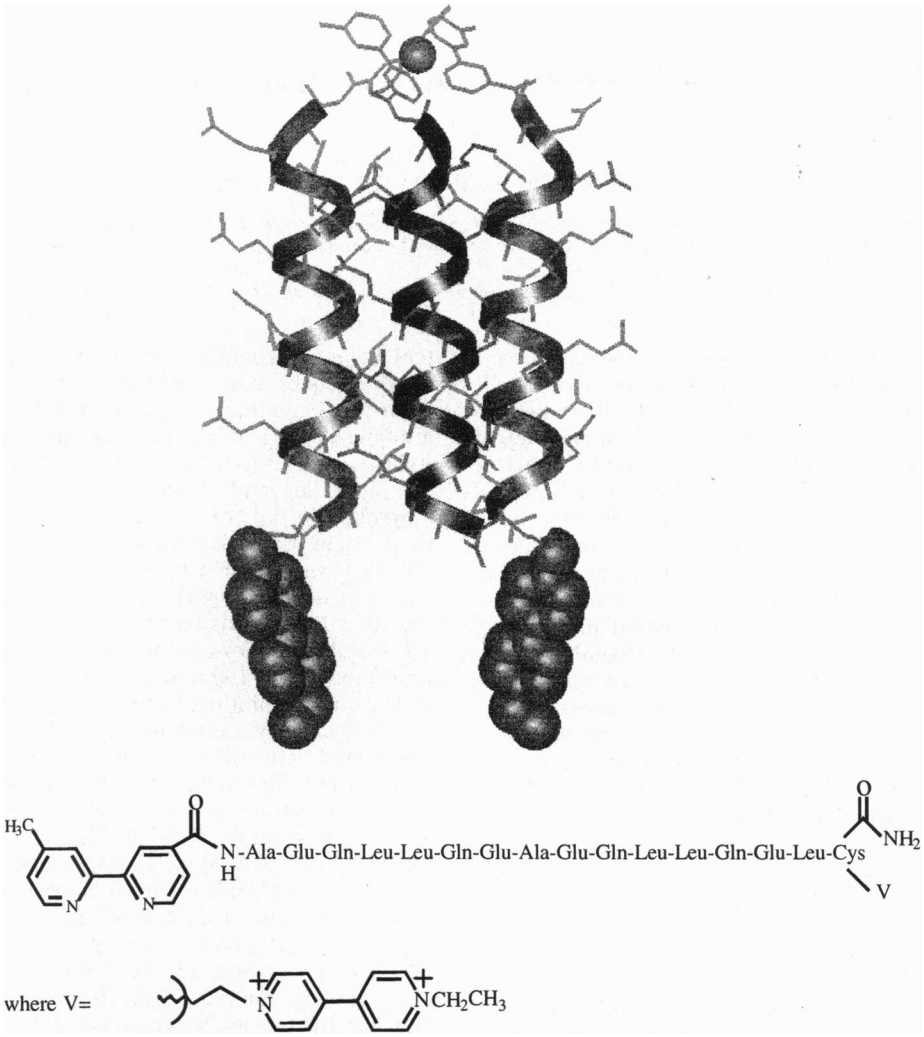

FIG. 1. Composition of the 16-mer synthetic peptide used to form the trimer and a computer model of the three helix bundle used in these studies. The N-terminal metal center is at the top, with the C-terminal viologens represented in space-filled format. V is viologen, the trivial name of the C-terminal modifier, 1-ethyl-1′-ethyl-4,4′-bipyridinium.

estimate the potentials because of the tendency of the metalloprotein to foul the electrode.

Synthesis of Co^{III}(4-Methyl-4′-alanine-2,2′-bipyridine)$_3$. The synthesis of this model compound followed the procedure described above for Co^{III}(16-mer)$_3$-viologen. The formation of the product was confirmed by absorbance spectroscopy and cyclic voltammetry. Formation of 4-methyl-4′-alanine-2,2′-bipyridine was confirmed by HPLC and mass spectroscopy.

Synthesis of Ru^{II}(16-mer)$_3$-5-({[(2-Acetyl)amino]ethyl}amino)naphthalene-1-sulfonic Acid (Ru tris(16-mer)-AEDANS). Formation of Ru^{II}(16-mer)$_3$ followed a literature procedure (9). 5-((((2-Iodoacetyl)amino)ethyl)amino)napthalene-1-sulfonic acid (IAEDANS) was purchased from Molecular Probes and used to modify the C terminus of the bundle by means of an SN2 displacement of the iodine by the thiol group of cysteine. Conditions for the modification are similar to the viologen modification of the peptide. The final Ru^{II}(16-mer)$_3$-AEDANS product was purified by reverse-phase HPLC using a Vydac C-18 column. A linear gradient of 25–60% CH_3CN in H_20 over 35 min was used. The buffer solutions were 0.02 M in triethylamine (pH 6.5). The final product elutes at 52% CH_3CN. Formation of the product was confirmed by ultraviolet-visible absorption spectroscopy, fluorimetry, and mass spectroscopy. $\lambda(\varepsilon, M^{-1}\,cm^{-1}) = 472\ (9.8 \times 10^4)$ is comparable to that of Ru^{II}(bipyridine)$_3$ (16). Errors in the extinction coefficients are estimated to be ±10%.

Pulse Radiolysis. All radiolysis experiments were performed on the Van de Graaf accelerator at the Brookhaven National Laboratory. The dosage was controlled so that, typically, less than 20% of the reactants were reduced during a single shot. Transient absorbance signals were monitored in a similar arrangement to the photolysis experiments. Signals were processed with a Lecroy 6810 recorder, and the data were analyzed on a microcomputer. All samples were thoroughly purged with N_2O, which reacts with the aqueous electron to form the hydroxyl radical. The reducing carbon dioxide radical is then formed from the reaction of the hydroxyl radical with formate ion present in the buffer. The carbon dioxide radical was used because it is a more selective reductant than the aqueous electron. Data are the result of at least three shots at three or more concentrations.

Flash Photolysis. Laser flash photolysis experiments were carried out using an excimer Lambda Physik Lextra 50, XeCl, 308 nm as the excitation source. Transient absorbance signals were monitored at right angles to the excitation with a conventional xenon or tungsten lamp, monochromator, photomultiplier tube arrangement. The signal from the photomultiplier was recorded and digitized with a Tektronix TDS 620 digitizing oscilloscope and then passed to a microcomputer for storage and analysis. Appropriate long-pass filters were placed

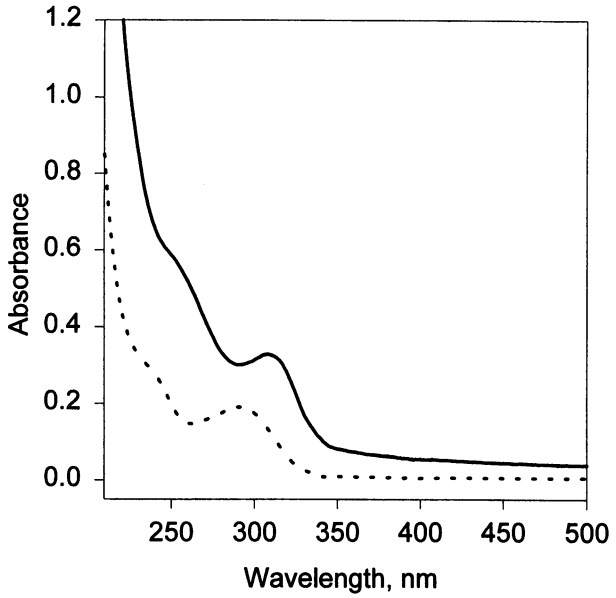

FIG. 2. Absorption spectra of 20 μM 16-mer-viologen (dotted line) and 41 μM Co^{III}(16-mer)$_3$-viologen (solid line) in 100 mM phosphate (pH 7.0), showing the shift in the bipyridine absorbance maxima from 292 to 308 nm.

on either side of the sample to prevent analyzing light from escaping. All samples were argon-purged for at least 10 min. The photoreduction chemistry of viologen has been described (17). Data are the result of at least three shots at three or more concentrations.

Protein Conformation. CD measurements were made on a Jasco 710 spectropolarimeter using 0.1-, 0.5-, and 1.0-mm water-jacketed Hellma cells at 25°C. Concentrations of the samples were varied between 1 and 0.01 mM. Protein concentrations were determined by ultraviolet-visible absorbance spectroscopy and amino acid analysis (Waters). The degree of

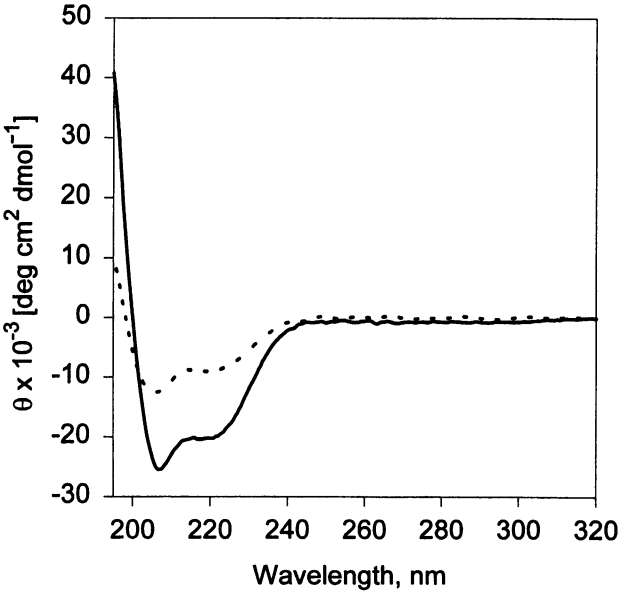

FIG. 3. Molar ellipticity per residue for 20 μM Co^{III}(16-mer)$_3$-viologen in 100 mM sodium formate, 50 mM sodium phosphate, 1 M ethanol, 100 mM triethanolamine (pH 7.0) (dotted line), and 20 μM Co^{III}(16-mer)$_3$-viologen in the same buffer with 25% trifluoroethanol (solid line). The CD in 6 M urea could only be recorded to 208 nm because of absorbance of the buffer and is not shown here. For the measurements, 0.01-mm pathlength cells were used. Data are the average of at least 30 scans. Estimated error in helicity is ±5% SD.

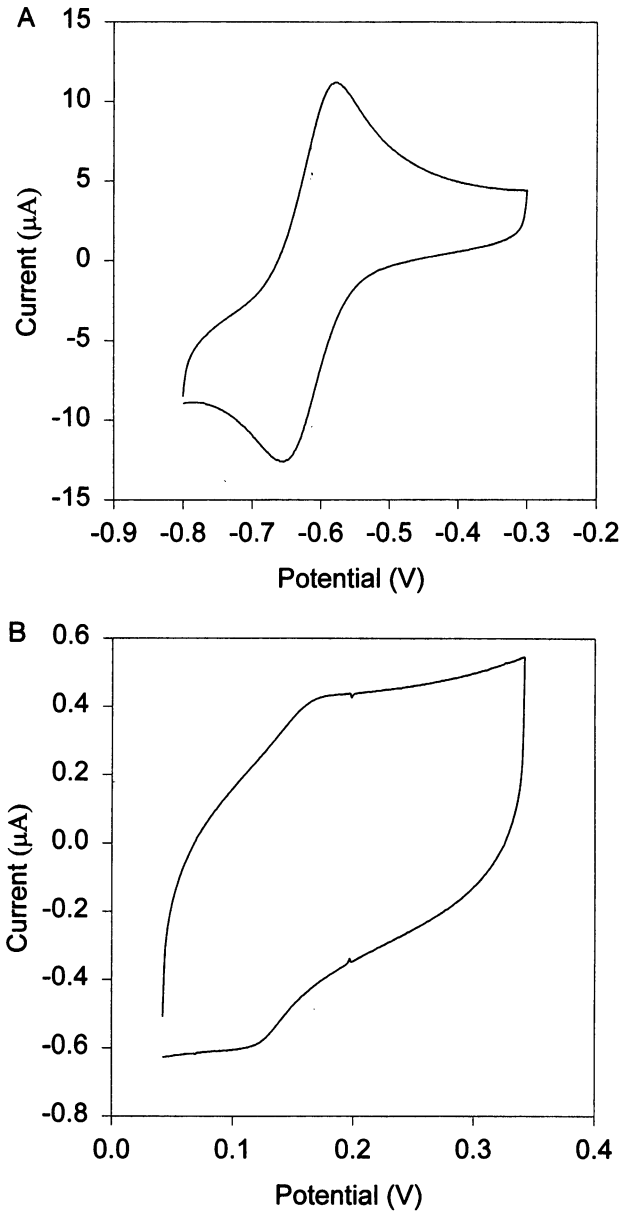

FIG. 4. Direct current cyclic voltammetry of (*A*) 80 μM 16-mer viologen in 100 mM sodium formate/50 mM sodium phosphate and (*B*) an approximately 55 μM Co^{III}(4-methyl-4′-alanine-2,2′ bipyridine)$_3$ in the same buffer, scan rate = 50 mV/sec. Saturated NaCl calomel electrode was used as a reference electrode.

α-helicity of the metalloprotein was estimated by means of the molar ellipticity per residue at 222 nm. A value of $[\theta]_{222}$ = −32,000 deg·cm^2·dmol^{-1} = 100% helicity was used (18).

Molecular Modeling. Insight II software [Biosym Technologies (San Diego)/Molecular Simulations (Waltham, MA)] was used on an Indigo 2 (Silicon Graphics, Mountain View, CA) computer.

Cyclic Voltammetry. A Cypress Systems (Lawrence, KS) CYSY-1 electroanalysis system was used for all measurements. The working electrode was a 3.0-mm gold disc (BAS, West Lafayette, IN), the reference electrode was a saturated NaCl calomel electrode (Corning), and the auxiliary electrode was platinum wire. When necessary, solutions were purged with argon.

Fluorescence Measurements. Commercially available instrumentation and software (PTI, South Brunswick, NJ) were used for both steady-state and time-resolved fluorescence measurements.

Absorption Spectroscopy and Amino Acid Analyses. A Perkin–Elmer Lambda 6 double-beam instrument was used to estimate optical densities. The extinction coefficients for the metalloproteins were based on known extinction coefficients for the unmodified 16-mer peptides that were determined by means of quantitative amino acid analysis in triplicate at the Cornell University Biotechnology Program. The determinations were performed by Robert Sherwood.

$$e^-(2MeV) \xrightarrow[N_2O/HCO_2Na]{H_2O} CO_2^- \text{ (6 per 100 eV absorbed)}$$

$$CO_2^- + Co^{III}(16\text{-mer})_3V^{2+} \begin{cases} \nearrow\ Co^{III}(16\text{-mer})_3V^{+}\cdot \\ \downarrow k_{et} \\ \searrow\ Co^{II}(16\text{-mer})_3V^{+2} \end{cases}$$

Scheme I

Kinetics measurements. The radiolysis experiment proceeds via the following:
where V refers to viologen in the scheme.

$$Co^{III}(16\text{-mer})_3V^{2+} \xrightarrow{hv,\ TEOA} Co^{III}(16\text{-mer})_3V^{+}\cdot$$

$$Co^{III}(16\text{-mer})_3V^{+}\cdot \xrightarrow{k_{et}} Co^{II}(16\text{-mer})_3V^{+2}$$

Scheme II

Flash photolysis. The photochemical experiment proceeds according to:
where TEOA is triethanolamine, used as a reductant.

RESULTS AND DISCUSSION

Flash photolysis and pulse radiolysis studies of $Co^{III}(16\text{-mer})_3$-viologen in aqueous solutions show a diffusion controlled reduction of the viologen chromophore, followed by exergonic ($\Delta G \approx -0.8$ eV) ET to the cobalt. The observed rate is independent of peptide concentration, laser pulse energy, or radiation dose, consistent with intraprotein ET along the helix. Rates of reactions were monitored at 600 and 370 nm for the viologen oxidation and at 320 and 308 nm to follow the chemistry of the Co^{III}(bipyridine)$_3$ moiety, respectively. Furthermore, all experiments were conducted under oxygen-free conditions, precluding the formation of disulfide bridges between unmodified cysteine residues. Since the chromophores have distinct absorbance maxima, changes in the absorbance will correspond to changes in concentration of reactants and products as determined by Beer's Law. Typical radiolytic data are shown in Fig. 5. In this experiment, time = 0 is defined when the absorbance of the viologen in its reduced state has reached a maximum. The prompt viologen reduction is several orders of magnitude faster than the electron transfer rate in the metalloprotein and thus provides a convenient starting point for the reaction.

Photolytic control experiments with 16-mer-viologen show only reduction of the viologen chromophore with no subsequent reaction. However, studies of the $Co^{III}(16\text{-mer})_3$-viologen complex reveal a reoxidation of the viologen complex, with concomitant reduction of the Co^{III}(bipyridine)$_3$ moiety. Photochemical data are shown in Fig. 6. As shown in Scheme II, TEOA was used as a reductant to increase the yield of reduced viologen in the experiment. The reduction of the viologen is complete within 9 ns and defines time = 0. In both radiolytic and photolytic experiments, the reoxidized viologen

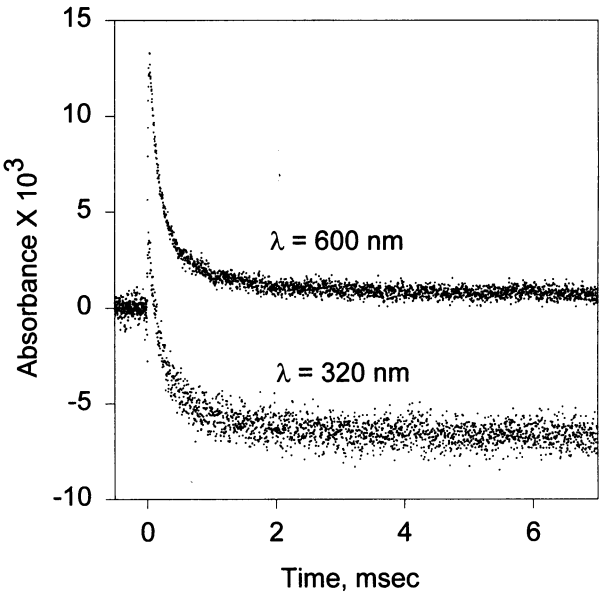

FIG. 5. Pulse radiolysis transient absorbance data for 0.5 μM $Co^{III}(16\text{-mer})_3$-viologen showing the decay at 600 nm due to oxidation of the viologen radical cation moiety and the bleach at 320 nm due to the reduction of the Co^{III} moiety. The initial rapid increase at 600 nm is due to the prompt reduction of viologen by CO_2^-. Solution conditions are given in Table 1.

is a stable product. However, $Co^{II}(16\text{-mer})_3$ is not inert and slowly decreased in concentration on a time scale of several minutes.

The role of conformational equilibria in protein-mediated ET was probed by inducing conformational extrema of the peptide using 6 M urea or 25% TFE and the results are given in Table 1. The metalloprotein unfolds in 6 M urea to produce a random coil structure (0% helicity). Alternatively, in the presence of 25% TFE, ≥75% helicity is obtained as shown by CD spectroscopy. When the folded and unfolded proteins are examined by pulse radiolysis and flash photolysis, a first order process is observed. However, studies of the 16-mer in the presence of 25% TFE yield a $k_{et} = 2000 \pm 200\ s^{-1}$, a >2-fold increase in the intramolecular ET rate compared with studies of the random coil configuration. Lastly, studies at low helicity (≤45%) yielded similar rates to the unfolded system, suggest-

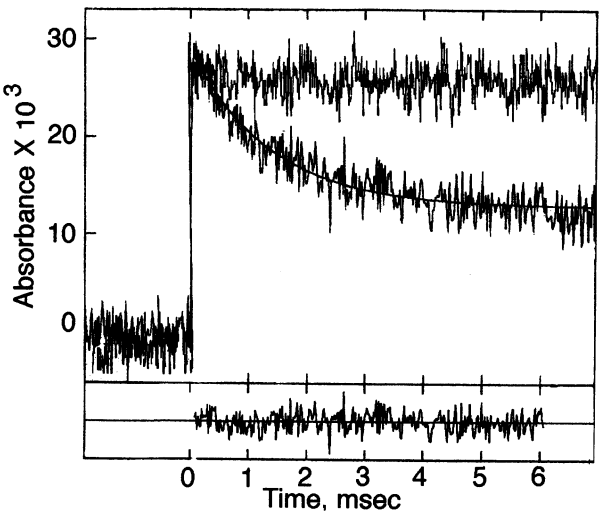

FIG. 6. Flash photolysis transient absorbance data for 1.2 mM 16-mer viologen (upper curve) and 12 μM $Co^{III}(16\text{-mer})_3$-viologen (lower curve) in 100 mM sodium formate, 50 mM sodium phosphate, 100 mM triethanolamine, 1 M ethanol (pH 7.0) at 600 nm.

Table 1. Comparison of the effects of solution conditions on helicity and ET rates

Experiment	% helicity	rate (s^{-1})
Pulse radiolysis*	45	$6.3 \pm 0.5 \times 10^2$
Flash photolysis†	28	$7.0 \pm 0.5 \times 10^2$
In 25% TFE†	77	$2.0 \pm 0.2 \times 10^3$
In 6 M urea†	0	$9.0 \pm 1.0 \times 10^2$

*All radiolysis experiments were carried out in 100 mM formate/50 mM phosphate (pH 7.0) and purged with N_2O.

†Laser flash photolysis was done in 100 mM formate/50 mM phosphate (pH 7.0)/100 mM triethanolamine/1 M ethanol. Solutions were purged with argon. Concentration of protein ranged from 80 μM to 0.5 μM.

ing that a higher degree of secondary structure is required to accelerate ET.

These rate changes cannot be accounted for by changes in either the reaction free energy or the reorganization energy, λ. The driving force for all solution conditions was identical: -0.79 ± 0.01 eV as estimated from cyclic voltammetry. In addition, changes in λ, as estimated from the dielectric continuum model (19), could at most account for a 10% change in the ET rate. This reflects the similar polarity of all solvent systems used. Therefore, the increase in the ET rate in the presence of 25% TFE must be explained by changes in H_{AB}, the electronic coupling between donor and acceptor, which in turn reflects the effective donor–acceptor distance.

To study the effects of solution conditions on R, the donor–acceptor distance, Förster energy transfer was used as a spectroscopic ruler according to

$$R = \left\{ \frac{(8.8 \times 10^{-28})\kappa^2 \phi_{em}}{n^4(\tau_o/\tau - 1)} \int F_D(\lambda)\varepsilon_A(\lambda)\lambda^4 d\lambda \right\}^{1/6},$$

where κ is the dipole–dipole orientation factor, ϕ_{em} is the fluorescence quantum yield of the donor, n is the index of refraction of the medium, and τ_o and τ are the emission lifetimes in the absence and presence of acceptor, respectively (20). For this experiment, Ru(16-mer)$_3$-AEDANS was used so that the AEDANS emission would overlap with the absorbance of the ruthenium moiety. The geometry of this bundle is identical to that of the Co^{III}(16-mer)$_3$-viologen system as determined by CD measurements. Moreover, the geometries of the Co^{III} and Ru^{II} moieties are known to be similar (21). Excitation in all experiments took place at 337 nm and the emission was monitored at 470 nm. κ^2 was estimated to be 2/3, $n = 1.4$, $\phi_{em} = 0.58$ and 0.64 in 6 M urea and 25% TFE, respectively.

A main source of error in Förster energy transfer experiments is the assignment of a value for κ^2, the geometric factor. A value of 2/3 is appropriate when the orientation of donor and acceptor are randomized on the time scale of the energy transfer. Because the energy acceptor moiety Ru^{II}(4-methyl-2,2′-bipyridine)$_3$ has effectively spherical symmetry, its geometry will be the same in all orientations with respect to the AEDANS moiety. Therefore, $\kappa^2 = 2/3$ is the correct value for the geometric factor under all solvent conditions. Direct measurements of fluorescence polarization of <0.3 for the Ru^{II}(4-methyl-2,2′-bypridine) moiety in all three solvent systems confirm the assignment of this value (22).

The resulting data (Fig. 7) clearly show that there is a distribution of donor–acceptor distances for the metalloprotein in both 6 M urea or 25% TFE with average R values of 18.5 and 17.8 Å, respectively. These distances are consistent with a conformation in which the AEDANS moiety is oriented parallel to one helical axis of the trimer. The distribution of distances can be explained by the flexible linker used to attach the energy donor to the metalloprotein, but may also be due to flexibility in the bundles themselves. Moreover, the data

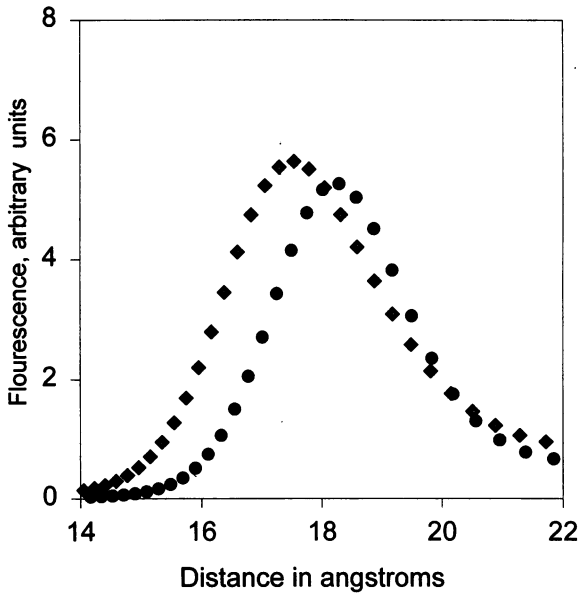

FIG. 7. Distributional fluorescence lifetime fit for RuII(16-mer)$_3$-AEDANS. One hundred exponentials were used yielding χ^2 values of 0.94 and 0.82 for experiments run in 6 M urea (solid circles) or TFE (diamonds), respectively.

show that the helical metalloprotein has a higher population of conformers with a smaller R than the same protein under denaturing conditions. The apparent 0.7 Å decrease in donor–acceptor distance in the helical conformation is self-consistent with the observed increase in the ET rate: using the well-established exponential dependence of the rate on the donor–acceptor distance $k_{ET} \propto \exp -(\beta R)$ with β, the electronic coupling factor, = 1.1 $Å^{-1}$ (23), and $\Delta R = 0.7$ Å, the predicted $k_{helix}/k_{random\ coil}$ is 2.2, in good agreement with the experimental $k_{helix}/k_{random\ coil}$ of 2.2.

We conclude that the stable triple-helix maquette of Ghadhiri (2) and Sasaki (10, 11) can indeed be elaborated to produce bifunctional redox proteins, which can translocate electrons across significant distances at physically reasonable rates. Moreover, due to their conformational variability under different solution conditions, such systems represent a means to investigate effects of helical conformation on rates of ET. The data unambiguously show an increase in the ET rate upon increase of the α-helical content of the Co^{III}(16-mer)$_3$-viologen metalloprotein. Additionally, the ET rates are consistent with the measured changes in donor–acceptor distances determined from Förster energy transfer experiments. These observations, which include the first electron transfer rates published for a purely *de novo* designed metalloprotein, set the stage for systematic studies of structural determinants of ET within a single, variable maquette.

We would like to thank Prof. C. Michael Elliott for many helpful discussions. The work at Brookhaven National Laboratory was carried out under contract DE-AC02-76H00016 with the U.S. Department of Energy and supported by its Division of Chemical Sciences, Office of Basic Energy Research. This work was also supported by National Institutes of Health Grant GM50019.

1. Handel, T. M., Williams, S. A. & DeGrado, W. F. (1993) *Science* **261**, 879–885.
2. Case, M. A. & Ghadhiri, M. R. (1993) *Angew. Chem. Int. Ed. Engl.* **32**, 1594–1597.
3. Vassilian, A., Wishart, J. F., van Hemeryck, B., Schwarz, H. & Isied, S. (1990) *J. Am. Chem. Soc.* **112**, 7278–7286.
4. Choma, C. T., Lear, J. D., Nelson, M. J., Dutton, P. L., Robertson, D. E. & DeGrado, W. F. (1994) *J. Am. Chem. Soc.* **116**, 856–865.

5. Therien, M. J., Bowler, B. E., Selman, M. A., Gray, H. B., Chang, I.-J. & Winkler, J. R. (1991) in *Electron Transfer in Inorganic, Organic and Biological Systems*, eds. Bolton, J. R., Mataga, N. & McLendon, G. (ACS, Washington, DC), pp. 191–199.
6. Geren, L., Hahm, S., Durham, B. & Millett, F. (1991) *Biochemistry* **30,** 9450–9457.
7. Isied, S., Ogawa, M. Y. & Wishart, J. F. (1992) *Chem. Rev.* **92,** 381–394.
8. Cabana, L. A. & Schanze, K. (1990) in *Electron Transfer in Biology and the Solid State*, eds. Johnson, M. K., King, R. B., Kurtz, D. M., Kutal, C., Norton, M. L. & Scott, R. (ACS, Washington, DC), pp. 101–124.
9. Ghadiri, M. R., Soares, C. & Choi, C. (1992) *J. Am. Chem. Soc.* **114,** 825–831.
10. Lieberman, M. & Sasaki, T. (1991) *J. Am. Chem. Soc.* **113,** 1470–1471.
11. Lieberman, M., Tabet, M. & Sasaki, T. (1994) *J. Am. Chem. Soc.* **116,** 5035–5044.
12. Fields, G. B. & Noble, R. L. (1990) *Int. J. Peptide Res.* **35,** 161–214.
13. Telser, J., Cruickshank, K., Schanze, K. & Netzel, T. L. (1990) *J. Am. Chem. Soc.* **111,** 7221–7226.
14. Bruinink, J., Kregting, C. G. & Ponjeé, J. J. (1977) *J. Electrochem. Soc.* **124,** 1854–1858.
15. Jackman, R. & Rillema, D. P. (1989) *J. Chem. Educ.* **66,** 343.
16. Durham, B., Caspar, J. V., Nagle, J. K. & Meyer, T. J. (1982) *J. Am. Chem. Soc.* **104,** 4803–4810.
17. Hoffman, M. R., Prasad, D. R., Jones, G. & Malba, V. (1983) *J. Am. Chem. Soc.* **105,** 6360–6362.
18. Chen, Y., Yang, J. & Chau, K. (1974) *Biochemistry* **13,** 3350–3359.
19. Marcus, R. A. (1965) *J. Chem. Phys.* **43,** 58–61.
20. Förster, T. (1959) *Discuss. Faraday. Soc.* **27,** 7–17.
21. Brunschwig, B. S., Creutz, C., Macartney, D. H., Sham, T.-K. & Sutin, N. (1982) *Faraday Discuss. Chem. Soc.* **74,** 113–127.
22. Haas, E., Katzir, E.-K. & Steinberg, I. (1978) *Biochemistry* **17,** 5064–5070.
23. Langen, R., Chang, I.-J., Germanas, J. P., Richards, J. H., Winkler, J. R. & Gray, H. B. (1995) *Science* **268,** 1733–1735.